Electronic Supplementary Material (ESI) for Materials Horizons.

Methods, supplementary figures and tables

Hydrogen Bonding to Oxygen in Siloxane Bonds Drives Liquid Phase Adsorption of Primary Alcohols in High-Silica Zeolites

Sambhu Radhakrishnan[a,b], Charlotte Lejaegere[b], Karel Duerinckx[a,b], Wei-Shang Lo[c], Alysson F. Morais[a,b], Dirk Dom[a,b], C. Vinod Chandran[a,b], Ive Hermans[c], Johan A. Martens[a,b] and Eric Breynaert*[a,b]

Contents

1. Methods 1
1.1. Sample preparation 1
1.2. Characterization 2
1.2.1. Solid state NMR 2
1.2.2. Infrared spectroscopy 2
1.2.3. Adsorption isotherm 3
2. Supplementary figures and tables 3
2.1. Synthesis compositions and obtained crystalline phases 3
2.2 NMR investigation of adsorption *in situ* in a rotor and peak assignments 8
2.3 Determination of maximum theoretical alcohol adsorption capacity in MFI zeolite framework 9
2.4 NMR spectral decomposition and mechanistic studies 10
2.5 NMR spectral decomposition and mechanistic studies 13
3. References 14

1. Methods

1.1. Sample preparation

Five ZSM-5 (MFI framework type) zeolite samples in ammonium form were obtained from Zeolyst. Herein they are dubbed according to their Si/Al ratio (MFI-11.5 (CBV2314), MFI-15 (CBV3024), MFI-25 (CBV5524), MFI-40 (CBV8014) and MFI-140 (CBV28014)). Before use, the powders were converted to the acid form by calcination at 550 °C. Properties of interest are listed in Table 1. Nitrogen physisorption data was recorded on a Micromeritics instrument (Tristar Surface Area and Porosity Analyzer). The samples were pretreated by heating the powders to 400 °C (ramp of 5 °C/min) under N_2 atmosphere using the SmartPrepTM Programmable Degas System (Micrometrics). The concentration of Brønsted acid sites and defect sites was estimated using NMR spectroscopy (Table 2). The chemical shift ranges of ^{1}H NMR resonances used for integration of silanol, aluminol and bridging hydroxyl groups were 1 – 2.5, 2.5 – 3.5 and 3.5 - 7 ppm, respectively (Figures S1 and S2, Table S1 and S2).[1] The quantification may be slightly influenced by the presence of trace amounts of very strongly adsorbed water that could not be evacuated by dehydration treatment at 200 °C at 75 mTorr and also by chemical exchange effects[2] (Table 2 and Figure S1). Spectral

decomposition of ^{27}Al direct excitation spectra using Czjzek[3] line-shapes for quadrupoles in DMFIT software was used for identification and quantification of ^{27}Al species in different coordination environments, namely tetra-, distorted tetra-, penta- and hexa-coordination (Table 1, Table S3 and Figure S3). The presence of significant amounts of extra-framework aluminum was observed, especially in the case of Al-rich zeolites (MFI-11.5, MFI-15), accounting for the higher concentrations of aluminols.

1.2. Characterization

1.2.1. Solid state NMR

^{1}H direct excitation, ^{1}H-^{13}C CPMAS and ^{1}H-^{29}Si HETCOR spectra were acquired on a Bruker Avance III 500 MHz (11.7 T) spectrometer equipped with a 4 mm H/X/Y triple resonance solid-state magic angle spinning (MAS) probe. Adsorbent samples were packed into a 4 mm ZrO_2 rotor and dried inside the rotor for 16 h at 200 °C under vacuum (75 mTorr). The dried adsorbents were subsequently loaded with alcohol, followed by capping the rotors with vespel snap-on caps and equilibrated for 4 h at 60 °C prior to the measurement. ^{1}H direct excitation spectra were recorded in a quantitative way[4] with a π/2 radio-frequency pulse (RF) at 83 kHz, averaging 8 transients with a recycle delay of 2 s. ^{1}H–^{1}H double-quantum–single-quantum (DQ–SQ) MAS correlation spectra were measured using the BABA[5–7] sequence with excitation and conversion periods of 0.13 ms. The two-dimensional spectra were collected with 80 t_e increments of 66.67 µs in the indirect dimension and 16 transients in the direct dimension. ^{1}H-^{13}C (125.95 MHz) cross-polarization (CP) MAS NMR experiments were recorded at a MAS rate of 15 kHz using a 83 kHz ^{1}H excitation pulse, a 2500 µs ramped pulse (100 % - 70 %), ^{1}H contact pulse at 50 kHz and a square ^{13}C contact pulse at 65 kHz, accumulating 2048 scans with a recycle delay of 2 s. ^{1}H-^{13}C CP-HETCOR experiment was performed at 15 kHz MAS using 64 scans and a contact time of 500 µs, collecting 144 slices with 16.67 µs increment. SPINAL-64[8] H-decoupling was performed during acquisition using 56 kHz RF pulses. ^{1}H and ^{13}C spectra were referenced using adamantane ^{1}H and ^{13}C (methylene) resonances at 1.81 ppm and 38.5 ppm respectively as a secondary reference to neat tetramethyl TMS (0 ppm). Direct excitation ^{29}Si (99.50 MHz) MAS NMR was performed at a MAS rate of 15kHz, using 61 kHz RF excitation pulses, 256 transients with a recycle delay of 120 s and SPINAL-64 ^{1}H-decoupling at 56 kHz. ^{1}H-^{29}Si CP-HETCOR experiment was performed at 15 kHz MAS using 160 scans and a contact time of 1000 µs, collecting 72 slices with 33.33 µs increment. ^{1}H contact pulse of 56 kHz (100 - 70 % ramped pulse) and a square 70 kHz RF on Si was used. SPINAL-64 ^{1}H decoupling with 56 kHz RF pulses were performed during acquisition. ^{29}Si spectra were referenced against neat TMS using secondary reference Q_8M_8 $[Si(CH_3)_3]_8Si_8O_{20}]$ resonance at 109.68 ppm, for the farthest downfield frequency peak.[9] ^{27}Al direct excitation NMR spectra were acquired at 15 kHz MAS using 208 kHz RF pulse, recycle delay of 1 s and SPINAL64 decoupling at 56 kHz RF. 4096 transients were acquired for MFI-11.5, MFI-15, MFI-25, MFI-40, while 49,152 transients were acquired for MFI-140. ^{27}Al spectra were referenced against a 1.1 M $Al(NO_3)_3$ solution in D_2O at 0 ppm. Spectral decomposition was performed with DMFIT[10] software.

1.2.2. Infrared spectroscopy

IR spectra of 1-pentanol adsorption on zeolites were recorded by using a Bruker Vertex 70 spectrometer equipped with a liquid nitrogen-cooled Mercury-Cadmium-Telluride (MCT) detector. The measurements were performed by averaging 128 scans at 4 cm^{-1} resolution between 800 and 4000 cm^{-1}. Zeolite powders (~10 mg) were pressed into a self-supporting wafer and placed into a sample holder in a home-built transmission cell. The temperature of the sample was controlled by a PID controller (LOVE Controls 16B) with a type-K thermocouple directly contacted with the sample holder. Before the IR measurements, each sample was heated up to 30 ºC under a dry air flow (40 cm^3 min^{-1}, Drierite Gas Purifier) for 12 h. The IR cell was heated up to 500 ºC (5 ºC min^{-1}) and held for 1 h under a dry air flow (40 cm^3 min^{-1}). After that, the cell was cooled down to 200 ºC under dry air and evacuated (< $1x10^{-4}$ Torr) by a turbo pump (Pfeiffer). A background FT-IR spectrum was collected at 30 ºC under vacuum (< $1x10^{-4}$ Torr). The zeolites were then exposed to increasing vapor pressures of 1-pentanol at 25 ºC to promote adsorption. Different pentanol dosages were achieved by bubbling N_2 through a bubbler (Aldrich, 4 mL) containing 1-pentanol and assuming saturation. For each 1-pentanol dosage, the IR spectrum was measured after the pressure in the cell remained constant for 3 min.

1.2.3. Adsorption isotherm

Liquid phase adsorption at high solid/liquid ratio. Determination of the saturation capacity of MFI-11.5 and MFI-140 for the different alcohols (methanol, ethanol, 1- propanol obtained from Acros Organic and 1-pentanol from Fluka Chemicals) and 1- pentanol adsorption on MFI-15, MFI-25 and MFI-40 was performed by addition of small aliquots of the alcohol to a rotor-packed zeolite dehydrated at 200°C under vacuum after packing in the NMR rotor. Adsorption of pure alcohol from the liquid phase onto MFI zeolite was investigated using *in situ* quantitative ^{1}H direct excitation MAS NMR.[4] ^{1}H direct excitation MAS NMR enables absolute quantification, [4,11,12] while at the same time allowing to discriminate between adsorbed and mobile fractions based on their relaxation behaviour. The combined information allows to quantify adsorption.

2. Supplementary figures and tables

2.1. Synthesis compositions and obtained crystalline phases

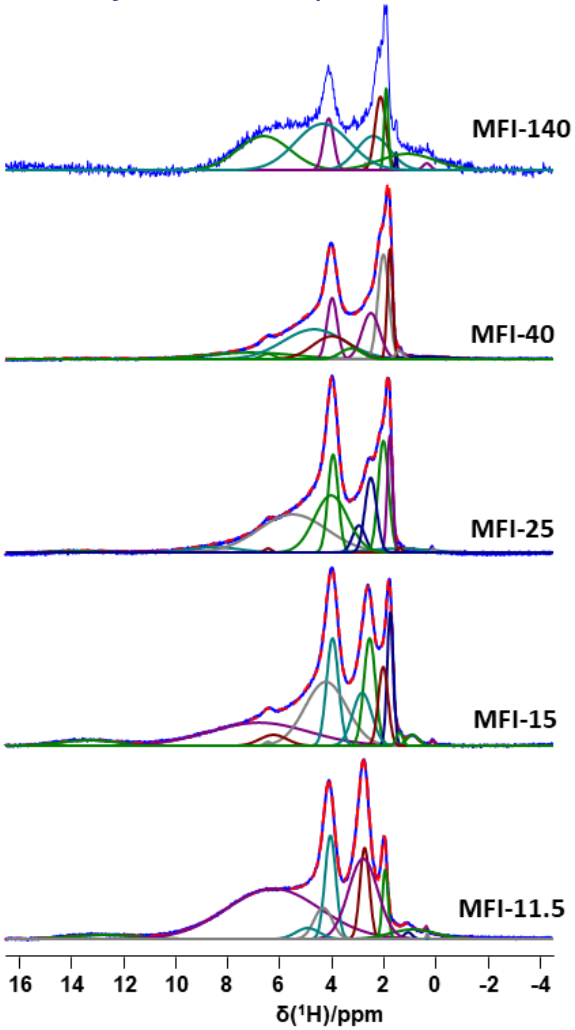

Figure S1. Spectral decomposition of ^{1}H NMR spectra of all the dehydrated adsorbents. All the spectra are scaled to height.

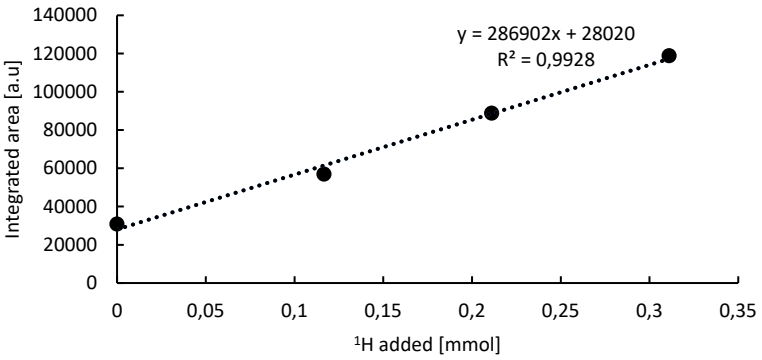

Figure S2. Integrated areas plotted against amount of ^{1}H added [mmol/g]. The slope of the fit (286902) is the area/mmol ^{1}H.

Table S1. Determination of concentration of different ^{1}H species (BAS/BAS+H_2O, AlOH & SiOH) in the different adsorbents. The adsorbents were dehydrated under vacuum (0.75 Torr) at 200°C. The slope of the standard addition curve (286902) was used for the calculation

		Relative Integral (%)			Concentration [mmol/g]		
Adsorbent	Total integral per gram	BAS/BAS+H_2O	AlOH	SiOH	BAS/BAS+H_2O	AlOH	SiOH
MFI-11.5	476257.3	60.2	36.7	3.0	1	0.61	0.05
MFI-15	289771	38.6	13.3	9.0	0.64	0.22	0.15
MFI-25	240997.7	36.1	2.4	12.0	0.6	0.04	0.2
MFI-40	172141.2	22.3	4.8	9.0	0.37	0.08	0.15
MFI-140	34428.24	4.2	0.6	2.4	0.07	0.01	0.04

Table S2. Experimental data of water standard addition to determine the integrated area/mmol ^{1}H. Integrated areas and amount of water added in g and as mmol are represented. Q-values of the NMR probe head was measured using a HP RF Network Analyzer

Water added [mg]	^{1}H added [mmol]	Area	Q-values
0.0	0.000	30824.68	620.9
1.1	0.117	56893.53	622.2
1.9	0.211	88801.32	596.9
2.8	0.311	118857.4	595.3

Table S3. Si/Al ratio for the MFI zeolites used in this study. Column 1: data provided by the supplier; Column 2: values calculated from elemental analysis (ICP-OES) and Column 3: values reported in the PhD thesis of A. Janda (University of Berkeley) for the same materials.[13]

Zeolite	**Si/Al (Zeolyst)**	**Si/Al (ICP)**	**Si/Al (ICP) PhD Thesis A. Janda**[13]
MFI-11.5	11.5	12.5	12.1 ± 1.7
MFI-15	15	17.8	16.5 ± 2.5
MFI-25	25	32	28.8 ± 4.4
MFI-40	40	50	43.7 ± 6.5
MFI-140	140	152	142 ± 48

Table S4. Determination of concentration of different ^{27}Al species via spectral decomposition in the different adsorbents.

Zeolite	δ_{Iso} (^{27}Al) (ppm)	C_Q (MHz)	dCS (ppm)	Relative integral (%)	Assignment
MFI-11.5	56.2	2.6	3.4	40	Tetra
	52.9	1.1	3.7	4	Tetra
	47.9	1.8	17.6	25	Distorted-Tetra
	30.1	2.0	20.4	12	Penta
	0.3	1.6	4.8	4	Hexa
	-3.5	1.8	22.7	15	Hexa
	-5.6	1.4	2.9	1	Hexa
MFI-15	56.3	2.5	2.7	45	Tetra
	53.3	1.4	3.3	9	Tetra
	47.6	1.9	15.6	20	Distorted-Tetra
	31.0	2.0	20.4	10	Penta
	1.0	2.5	3.8	5	Hexa
	-4.8	2.3	23.8	11	Hexa
MFI-25	57.1	2.2	2.8	53	Tetra
	54.3	1.1	3.7	20	Tetra
	49.6	2.7	22.4	20	Distorted-Tetra
	0.3	1.2	3.0	2	Hexa
	-3.4	1.7	15.7	5	Hexa
MFI-40	60.4	1.5	18.6	3	Tetra
	57.0	1.6	2.7	47	Tetra
	54.2	1.0	3.4	35	Tetra
	49.8	1.4	23.2	11	Distorted-Tetra
	-0.3	0.5	1.4	1	Hexa
	-2.1	1.6	12.7	3	Hexa
MFI-140	60.0	1.5	16.9	5	Tetra
	57.0	1.5	2.9	45	Tetra
	54.5	1.8	2.4	27	Tetra
	49.8	1.5	27.9	18	Distorted-Tetra
	-0.3	1.4	16.4	5	Hexa

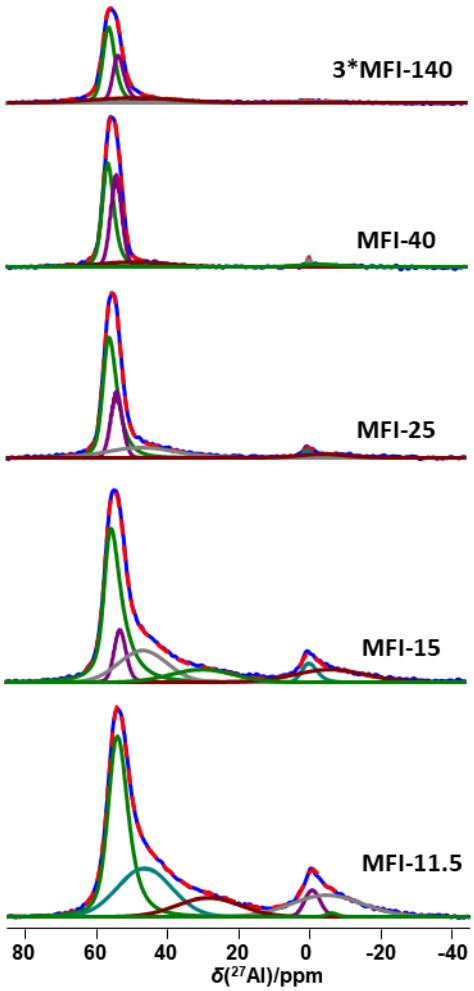

Figure S3. Spectral decomposition of ^{1}H decoupled ^{27}Al direct excitation NMR spectrum. Results depicted in Table 2.

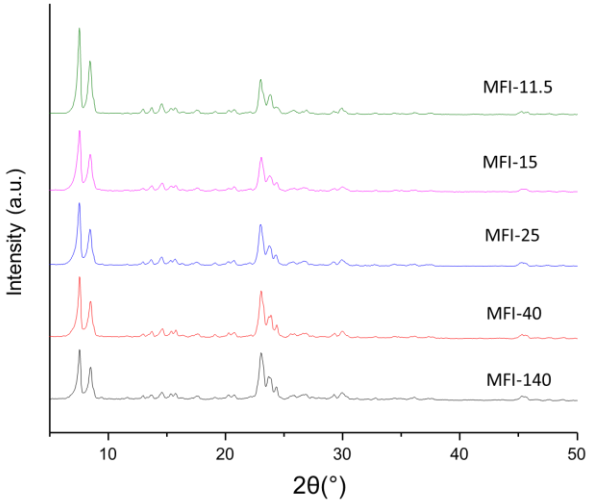

Figure S4. PXRD patterns of the different MFI zeolites,

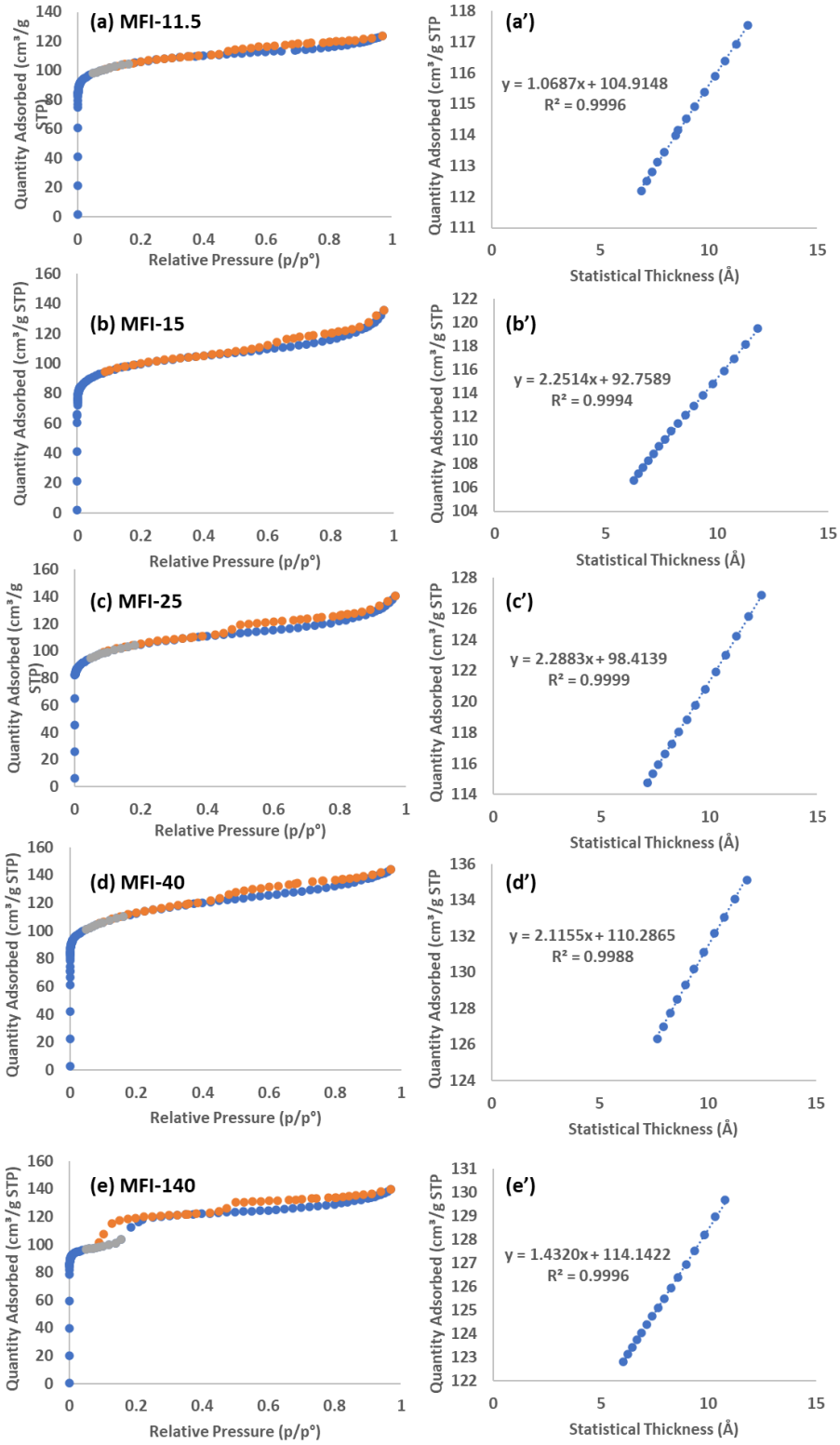

Figure S5. N_2 physisorption isotherm and t-plot respectively for H-MFI-11.5 (a, a'), H-MFI-15 (b, b'), H-MFI-25 (c, c'), H-MFI-40 (d, d') and H-MFI-140 (e, e').

2.2 NMR investigation of adsorption *in situ* in a rotor and peak assignments

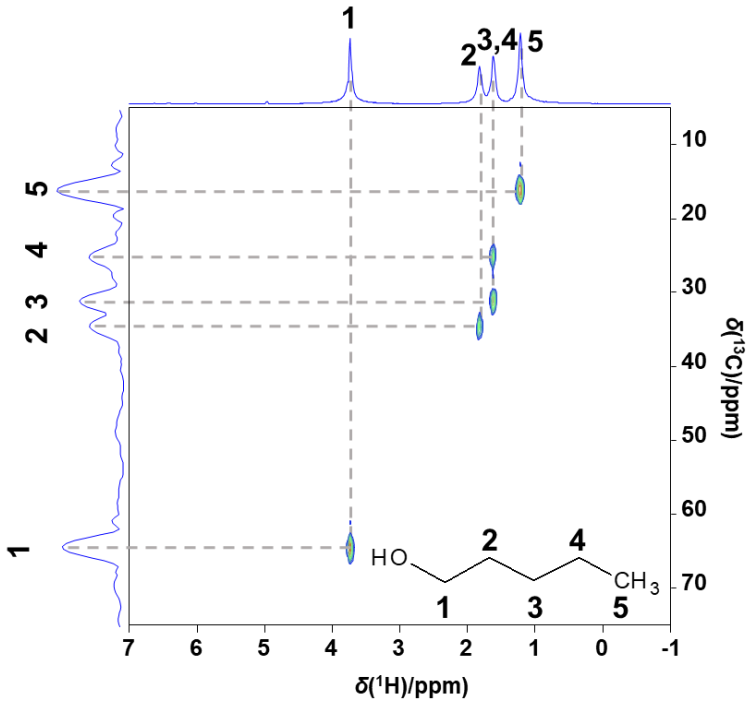

Figure S6. ^{1}H-^{13}C HMQC measurement of 1-pentanol liquid depicting the identification of different resonances

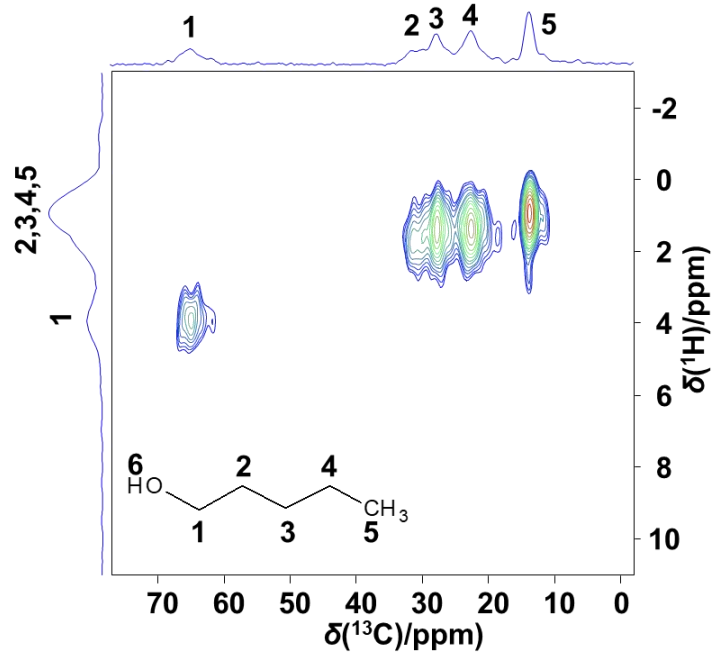

Figure S7. ^{1}H-^{13}C HETCOR spectrum of 1-petanol adsorbed on MFI-11.5, confirming the assignments.

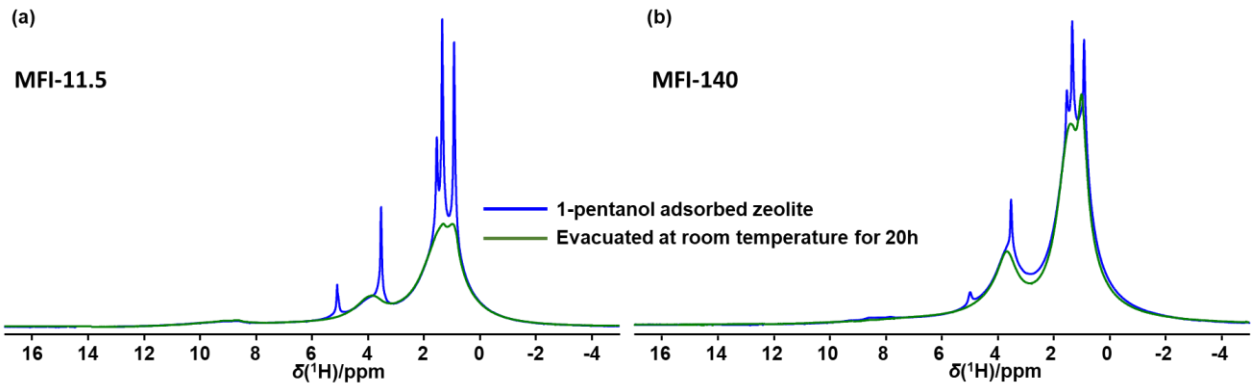

Figure S8. ^{1}H NMR spectra of MFI-11.5 (a) and MFI-140 (b) upon addition of 1-pentanol higher than the micropore volume (blue trace) and after evacuation at 0.75 Torr for 20 h (green trace).

2.3 Determination of maximum theoretical alcohol adsorption capacity in MFI zeolite framework

Theoretical maximum alcohol adsorption capacity per unit cell calculated by considering the geometry of the two-channel type MFI framework (Table 3, Table S4 and Figure S7). One unit cell contains four linear segments of 4.5 Å length, four sinusoidal segments of 6.5 Å length and four intersections, all of cross section 5.5 Å.[14] The total channel length considered for adsorption was 18, 26.6 and 22.4 Å for the straight channels, the sinusoidal segments, and the intersections respectively. Adsorbed alcohol molecules were assumed to exhibit a critical diameter of ~4.6 Å and to orient along the pore axis.[15] As expected from a geometrical perspective, increasing chain length leads to a decrease in the maximum number of adsorbed molecules.

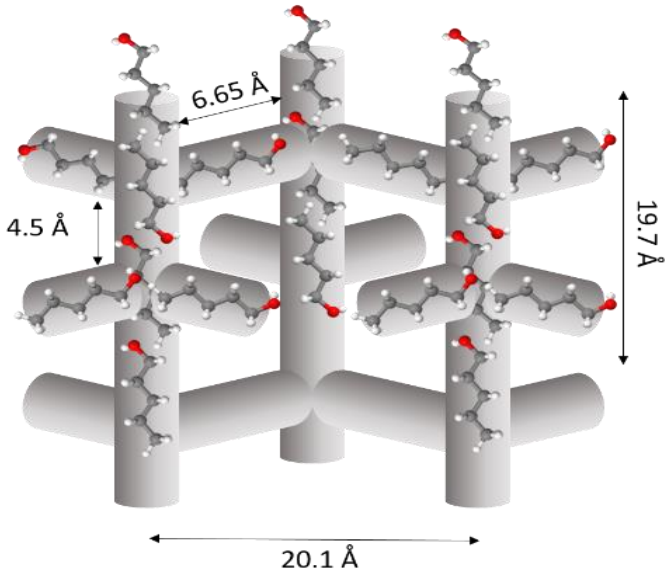

Figure S9. Visualization of the theoretical calculations of maximum pore filling of 1-pentanol in the MFI framework unit cell.[4,8]

Table S5. The molecule length and theoretical maximum adsorbed alcohol molecules per MFI unit cell[16,17]

1-Alcohol	Molecule length [Å]	Theoretical maximum MFI [N/UC]
Methanol	2.8	23.9
Ethanol	4.03	16.5
1-Propanol	5.31	12.5
1-Pentanol	7.07	9.5

Table S6. Variation of 1-pentanol adsorption capacity per BAS and per unit cell in the zeolite framework for MFI zeolites with different Si/Al ratios

Zeolite	*Adsorbed per UC*		*Adsorbed amount (mmol/g)*	*Adsorbed per BAS*	*Adsorbed per BAS + Defect sites*
	Theoretical	Experimental			
MFI-11.5	9.5	7.6	1.31	1.2	0.8
MFI-15	9.5	8.7	1.48	2.3	1.4
MFI-25	9.5	8.8	1.51	2.5	1.8
MFI-40	9.5	9.5	1.62	4.4	2.7
MFI-140	9.5	9.5	1.62	23.2	13.5

2.4 NMR spectral decomposition and mechanistic studies

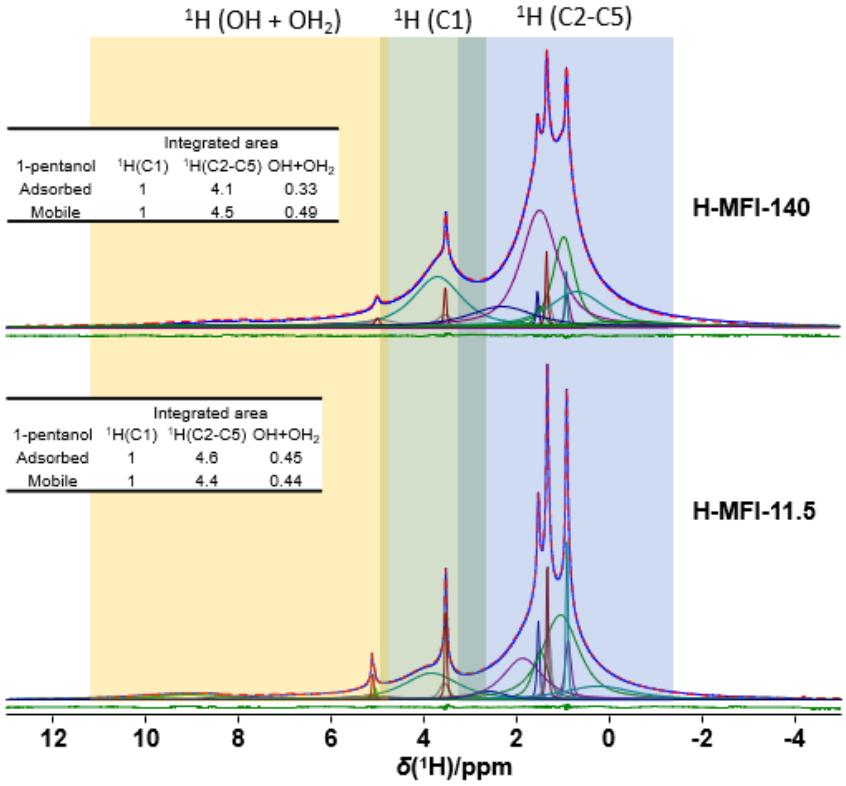

Figure S10. Spectral decomposition of ^{1}H direct excitation spectrum of 1-pentanol adsorbed H-MFI-140 and H-MFI-11.5 at 295K. Integrals relative to CH_2-1 ^{1}H resonance is provided in the table.

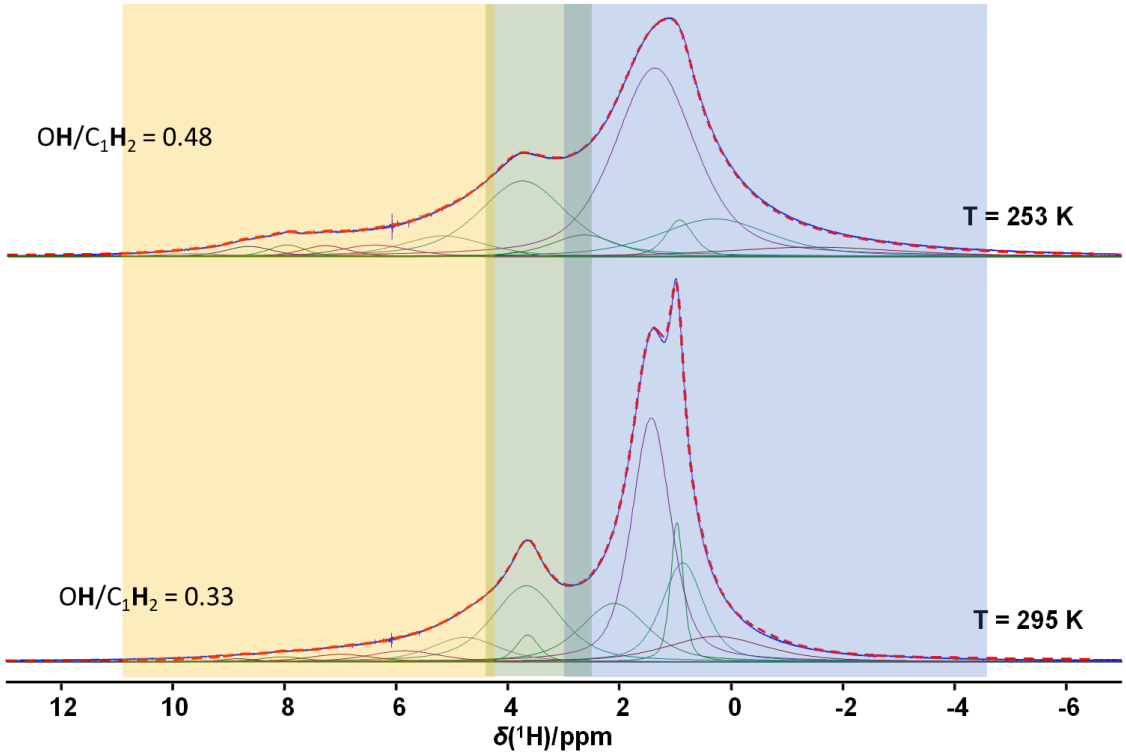

Figure S11. Spectral decomposition of ^{1}H direct excitation spectrum of 1-pentanol adsorbed H-MFI-140 at 295 K and 253 K. After adsorption exceeding the pore volume, the rotor with sample was subjected to vacuum treatment at room temperature to remove excess mobile molecules.

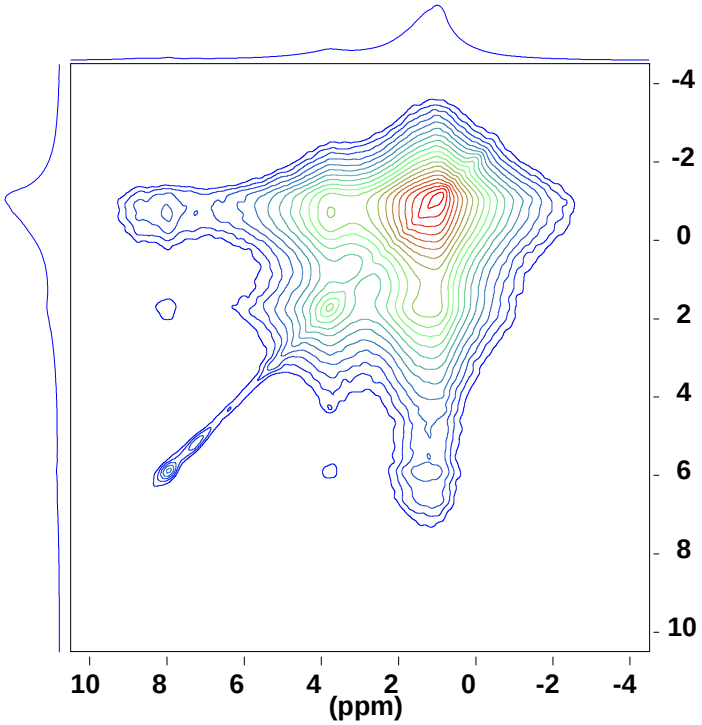

Figure S12: ^{1}H-^{1}H RFDR spectrum of 1-pentanol adsorbed H-MFI-140.

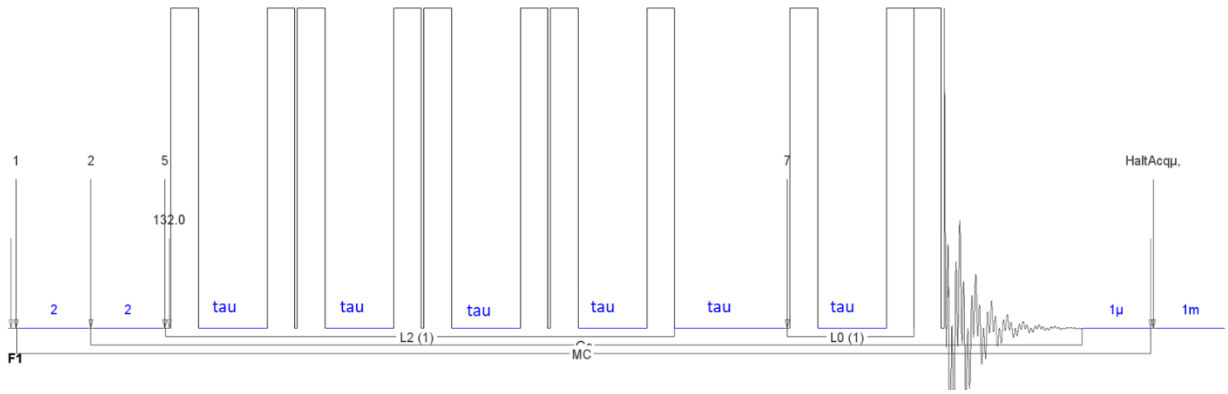

Figure S13. Pulse sequence (BABA) used for DQ-SQ experiments.

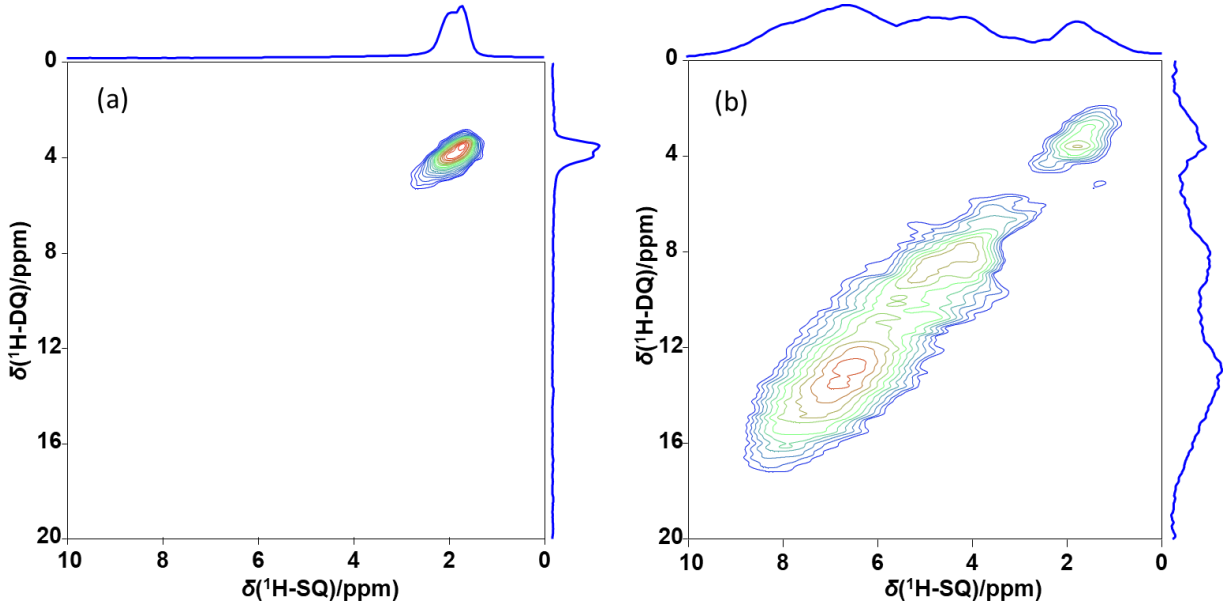

Figure S14. ^{1}H-^{1}H DQ-SQ spectrum of dehydrated H-MFI-140 (a) and H-MFI-140 with 10% pore-filling water. In the ^{1}H-^{1}H DQ-SQ spectra of the dry MFI-140 (Figure S14a), the self and cross correlations in and between the silanol nests immediately catch the eye of the reader (respectively at coordinates 1.8, 3.6 ppm and 2, 4 ppm). In the ^{1}H-^{1}H DQ-SQ spectra of the weakly hydrated (10% pore-filling) MFI-140 (Figure S14b), the self-correlations of silanol nests (1.8, 3.6 ppm), and multiple water populations [(4, 8 ppm) & (6.5, 13 ppm) , most probably water hydrogen bonded to and in chemical exchange with silanol groups, as well as water hydrogen bonded to BAS / siloxane bridges respectively] are indeed readily observed.

2.5 I*n situ* FT-IR investigation of 1-pentanol adsorption on MFI-11.5 and MFI-140.

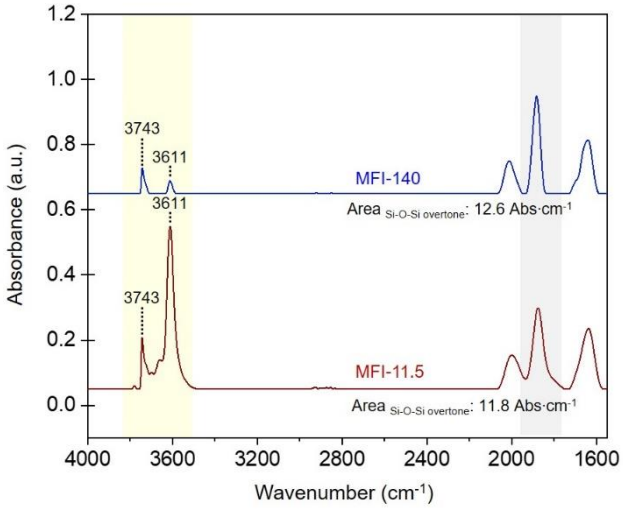

Figure S15. IR spectra of dehydrated MFI-140 and MFI-11.5 measured at 200 ºC under dried air.

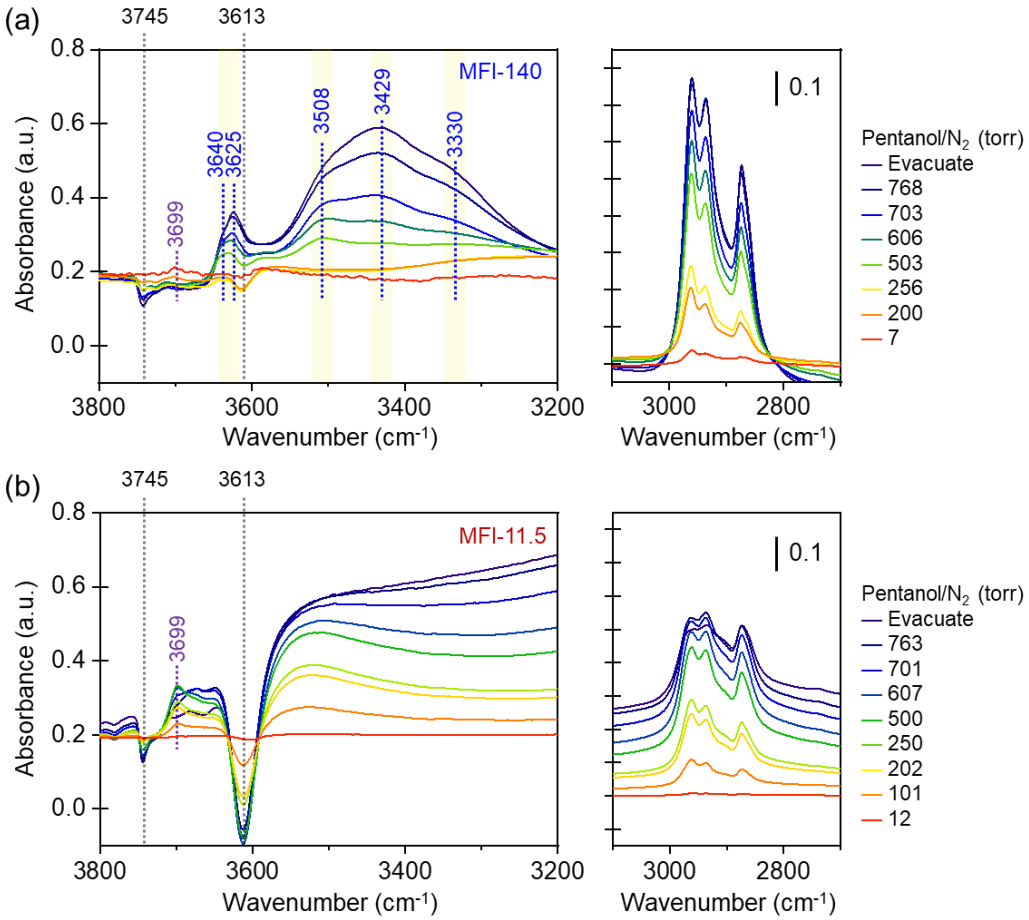

Figure S16. IR difference spectra of (a) MFI-140 and (b) MFI-11.5 with increasing dosage of 1-pentanol measured at 30 ºC. The background spectrum was collected on the parent sample at 30 ºC under vacuum.

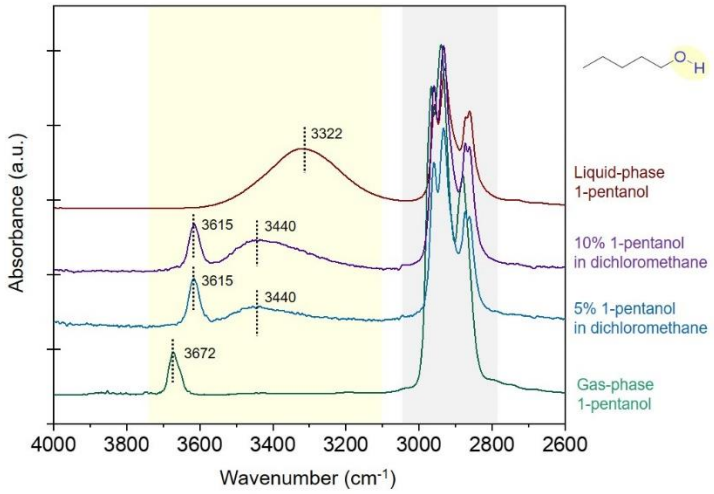

Figure S17. IR spectra of liquid-phase pentanol, gas-phase pentanol, and 1-pentanol dissolved in the nonpolar solvent of dichloromethane.

3. References

1 M. Hunger, *Catal. Rev. - Sci. Eng.*, 1997, **39**, 345–393.

2 M. Wang, N. R. Jaegers, M. S. Lee, C. Wan, J. Z. Hu, H. Shi, D. Mei, S. D. Burton, D. M. Camaioni, O. Y. Gutiérrez, V. A. Glezakou, R. Rousseau, Y. Wang and J. A. Lercher, *J. Am. Chem. Soc.*, 2019, **141**, 3444–3455.

3 J. B. d'Espinose de Lacaillerie, C. Fretigny and D. Massiot, *J. Magn. Reson.*, 2008, **192**, 244–251.

4 M. Houlleberghs, A. Hoffmann, D. Dom, C. E. A. Kirschhock, F. Taulelle, J. A. Martens and E. Breynaert, *Anal. Chem.*, 2017, **89**, 6940–6943.

5 M. Feike, D. E. Demco, R. Graf, J. Gottwald, S. Hafner and H. W. Spiess, *J. Magn. Reson. Ser. A*, 1996, **122**, 214–221.

6 S. H. Park, S. Radhakrishnan, W. Choi, C. V. Chandran, K. C. Kemp, E. Breynaert, R. G. Bell, C. E. A. Kirschhock and S. B. Hong, *J. Am. Chem. Soc.*, 2022, **144**, 18054–18061.

7 B. Vallaey, S. Radhakrishnan, S. Heylen, C. V. Chandran, F. Taulelle, E. Breynaert and J. A. Martens, *Phys. Chem. Chem. Phys.*, , DOI:10.1039/c8cp01586d.

8 T. Bräuniger, P. Wormald and P. Hodgkinson, *Monatshefte fur Chemie*, 2002, **133**, 1549–1554.

9 C. R. Pesce, G. L., Bowen and R. J. Rocha, J., Sardo, M., Allen, G. C., Walker, P. J., Denault, G., Serrapede, M., and Ball, *Clay Miner.*, 2014, **49**, 341–358.

10 D. Massiot, F. Fayon, M. Capron, I. King, S. Le Calvé, B. Alonso, J.-O. Durand, B. Bujoli, Z. Gan and G. Hoatson, *Magn. Reson. Chem.*, 2002, **40**, 70–76.

11 S. Radhakrishnan, H. Colaux, C. V. Chandran, D. Dom, L. Verheyden, F. Taulelle, J. Martens and E. Breynaert, *Anal. Chem.*, 2020, **92**, 13004–13009.

12 H. Vanderschaeghe, M. Houlleberghs, L. Verheyden, D. Dom, C. V. Chandran, S. Radhakrishnan, J. A. Martens and E. Breynaert, *Anal. Chem.*, 2022, **95**, 1880–1887.

13 A. L. Janda, University of California, Berkeley, 2015. https://escholarship.org/uc/item/27g1z5ck.

14 J. F. M. Denayer, K. De Meyer, J. A. Martens and G. V. Baron, *Angew. Chemie - Int. Ed.*, 2003, **42**, 2774–2777.

15 Z. Song, Y. Huang, W. L. Xu, L. Wang, Y. Bao, S. Li and M. Yu, *Sci. Rep.*, 2015, **5**, 13981.

16 E. García-Pérez, P. S. Barcia, J. A. C. Silva, A. E. Rodrigues and S. Calero, *Theor. Chem. Acc.*, 2011, **128**, 695–703.

17 H. Liu, Z. Zhang, B. H. Chen and Y. Zhao, *J. Porous Mater.*, 2008, **15**, 119–125.